

# QUANTIFICATION OF PHENOMENA OBSERVED DURING A SINGLE EVENT UPSET TEST ON A RECOVERABLE FLIGHT CONTROL COMPUTER

Matthew A. Ferguson, Undergraduate Student, Old Dominion University, Norfolk, VA  
Advisor: Linda Vahala, Ph.D., Old Dominion University, Norfolk, VA

## Abstract

This paper quantifies the phenomena observed during a Single Event Upset (SEU) test performed on a recoverable flight control computer (FCC) at Los Alamos Neutron Scattering Science Center (LANSCE). The FCC unit consisted of an Airplane Information Management System (AIMS) connected to a prototype roll-back recovery system. Both of these units were part of a larger closed-loop system controlled by a B737 flight emulator. Because of the high neutron flux at LANSCE, a very accelerated life test of the system was performed with a neutron energy spectrum similar to that which an operational aircraft would encounter during flight. The phenomena that were observed during the test included roll-back recoveries, operating system reboots, CPU idle periods with no I/O and loss of data synchronization within the computer. It is presumed that these phenomena were induced by the neutrons.

## Introduction

Reliability testing of microelectronics in harsh radiation environments is necessary to ensure the safe and reliable operation of systems that normally operate in such environments. Single event phenomena induced in avionics by cosmic radiation have been observed as far back as 1975<sup>1,2</sup>. In 1992, it was determined that the major source single event phenomena induced in aircraft electronics was due to atmospheric neutrons<sup>3</sup>.

Single event upsets are defined as "radiation-induced errors in microelectronic circuits caused when charged particles (usually from the radiation belts or from cosmic rays) lose energy by ionizing the medium through which they pass, leaving behind a wake of electron-hole pairs" [NASA Thesaurus - 914]. An easier description of the SEU could be that of a soft error that is induced by ionizing radiation which causes a transient fault in a system as indicated by a bit flip in digital media. Although there are many other types of radiation induced phenomena possible in microelectronic devices, this paper only assumes that the phenomena

observed during the test were induced by SEUs, or system response directly caused by the upsets.

Testing of microelectronic devices is normally done at the "chip" level to ensure that components used in systems are radiation hard before they are used in the system. The novelty behind this test is that it is a system level test, and the components are arranged in a fault tolerant design such that transient errors are detected and safe data is recovered. This particular system uses redundant components in a dual lock-stepped comparison architecture. This means that data is processed in parallel and compared at the same time in order to detect any errors that may have occurred as a result of a transient fault. If a miss-compare is observed at the output of the dual processors, then a roll-back recovery is performed which recovers "safe" data from a previous time.

The neutron environment at the LANSCE facility has been compared to the atmospheric neutron environment as modeled by Normand et al<sup>4</sup>, and is shown in Figure 1. This figure shows that the energy spectrum of the LANSCE facility is similar in shape to the normalized energy spectrum of the atmosphere at 34,000 ft. and 45° latitude. The atmospheric neutron flux was multiplied by  $2.62 \times 10^5$  for this comparison.

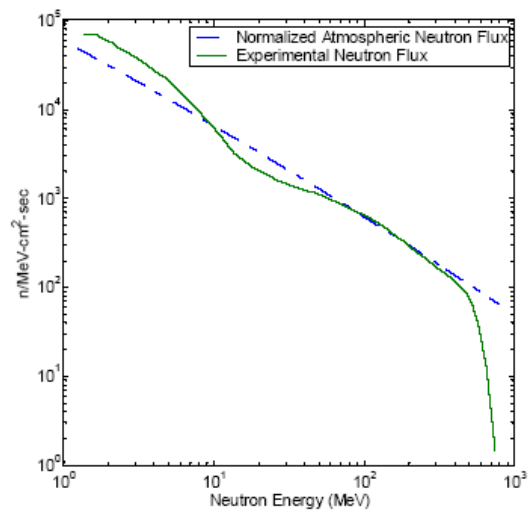


Figure 1: Atmospheric and LANSCE neutron energy spectrum

The use of the LANSCE facility allowed for performing an accelerated life test of the system, where 25 minutes of beam time was approximately equivalent to  $1.09 \times 10^5$  flight hours<sup>5</sup>. The neutrons were produced by running 800 MeV protons into a target. Charged particles produced in the spallation process were swept away by electro-magnets, leaving only neutral particles in the beam. The beam was then collimated by concrete blocks with circular paths cut through them. The nominal diameters of the collimators used for this test were 1", 2" and 3".

### Experiment

#### Set-up

During beam on conditions, only the FCC and prototype roll-back recovery unit were exposed to neutrons. In addition, the power supply board was removed from the FCC to allow for remote power control during the test to prevent component damage in the event of an over-current condition. Figure 2 shows the FCC/roll-back recovery system in the experimental hall at LANSCE. The foil covered device near the wall was a neutron counter used for providing indication that neutrons were present during the testing. The FCC and rollback recovery unit are shown on the table.



Figure 2: Experimental Set-up

Since the nominal beam diameters were much smaller than the surface area of any given side of the FCC, the experiment was broken down into objectives to target specific areas of digital components within the FCC. Figure 3 shows the three neutron flight paths used to isolate various components or groups of components during the experiment. Flight path

A was used for most of the runs as groups of components tended to be oriented across the circuit card assemblies (CCA). Flight path B provided for sampling across multiple groups of digital components, and Flight path C was used briefly to try to isolate individual components.

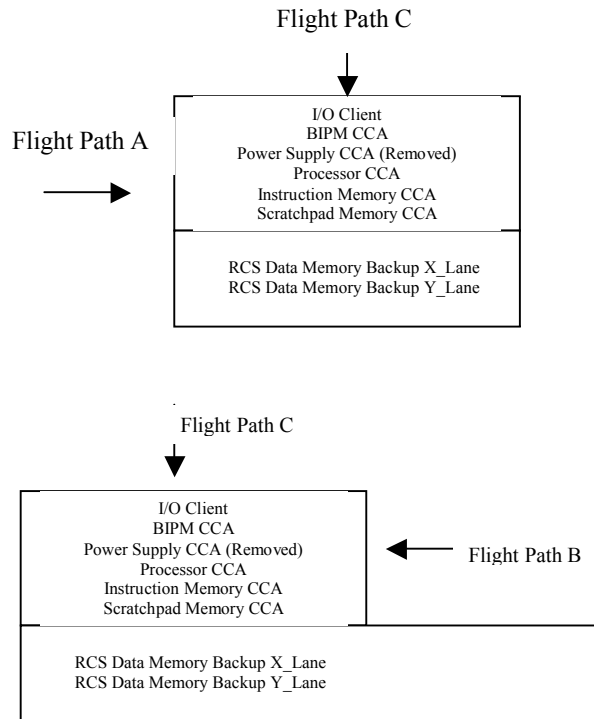


Figure 3: FCC Orientations with respect to beam

#### Targeting Objectives

Targeting objectives were initially chosen in order to maximize beam exposure to specific groups of complex digital components, while missing other groups of components. As time permitted, targeting objectives were expanded in order produce larger numbers of phenomena, and to try to isolate certain components within the FCC. Table 1 shows a summary of objective names, beam sizes, and the component groups of interest for each objective.

Objective Name	Beam Diameter (inch)/Flight Path	Component group(s)/CCA
T1	2"/A	RAM on Scratchpad Memory CCA
T2	2"/A	Processor #1 on Processor CCA
T2p	2"/A	Same as T2 for Processor #2
T2pp	3"/A	Both Processors
T2d1	1"/A	Processor #1 minimize exposure to other components
T3	2"/A	Flash memory on Instruction Memory CCA
T4	2"/B	Single CPU, RAM, Flash on respective CCAs
T4p	3"/B	Same as T4, but expanded to hit more components
T5	3"/B	Same as T4 expanded to include Rollback recovery components
T6	1"/C	Processor #1 through top of FCC to minimize exposure to other components
T6p	1"/C	Processor ASIC through top to minimize exposure to other components

Table 1: Targeting Objective Summary

In order to ensure each of the objectives were met, Fuji Film image plates were used to provide images and neutron intensity distributions both upstream and downstream of the FCC. These image plates worked on the principle of Photo-Stimulated Luminescence (PSL). In short, the image plates captured the integrated energy of the secondary ions produced by neutron interaction with surrounding materials. When the image plates were read, a laser stimulated the image plates to release light proportional to the number of neutrons that hit them. A more detailed discussion of how the images plates work can be found at reference 6.

LANL provided two image viewing applications, Rtif6 and IVW, to interpret the image plate data. Rtif6 provided neutron intensity distributions, and allowed for comparing data from multiple image plates. IVW allowed for interpreting image plate data as an x-ray image. Figure 4 shows an example of a neutron intensity distribution for a nominal 2" beam upstream of the FCC. Figure 5 shows the same beam downstream of the FCC after the neutrons have been scattered and attenuated in the device. These images were produced using Rtif6.

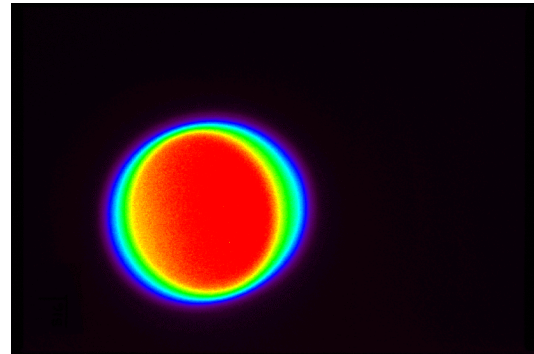


Figure 4: Nominal 2" beam intensity distribution upstream of the FCC

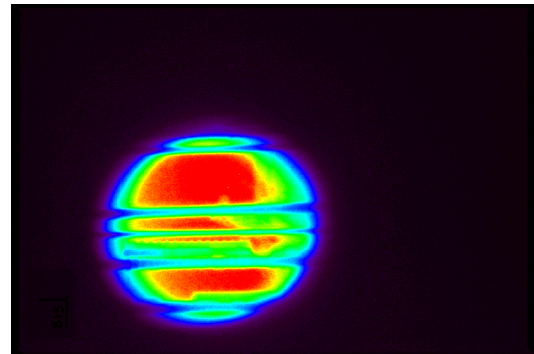


Figure 5: Nominal 2" beam intensity distribution downstream of the FCC

Figure 6 shows the same downstream data viewed with IVW as an x-ray image. The x-ray images were used to verify the objectives by transposing the images in the x-ray onto photos of circuit cards.

With a few exceptions, each of the objectives were met. The only exceptions were that during some targeting objectives, some complex digital components were inadvertently exposed when not intended.

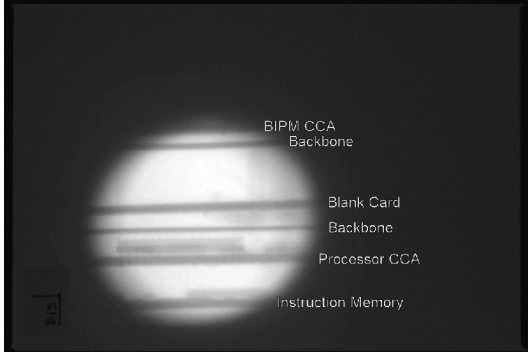


Figure 6: x-ray image view of same image plate data shown in Figure 5

### Results

Table 2 shows the run statistics for each targeting objective. The targeting objective identifiers are shown in bold. The number of runs corresponds to how many runs were made for a given objective. The total time indicates the time the beam was incident upon the FCC and the FCC was operating in either a normal or roll-back recovery condition. The remaining indicators are the number of occurrences each of the following phenomena were experienced in during the targeting objectives: (1) Roll-back Recovery, (2) Operating System Reboot, (3) Loss of I/O with CPU idle time, (4) Loss of synchronous communication between the FCC and the data acquisition equipment.

Integrated neutron intensities for neutron energies ranging between 1.5 MeV and 800 MeV were provided by LANL from their fission chamber. These data were extrapolated to the beam spot areas derived from the Full Width at Half Maximum (FWHM) measurements taken from the upstream image plates for each run. Figure 7 shows the FWHM measurement for the upstream image plate data shown in Figure 5. Extrapolations were made using equation (1). Solid angle data for each nominal beam size were provided by LANL.

$$(1) \quad \Omega = \frac{A}{r^2}$$

$\Omega$  = Solid Angle,  $A$  = Area,  $r$  = distance

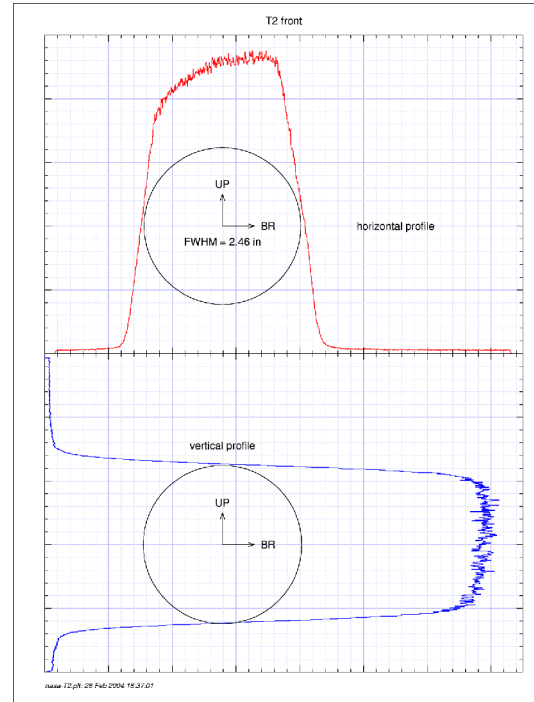


Figure 7: FWHM for a 2'' nominal beam obtained from the upstream image plate

	<b>T1</b>	<b>T2</b>	<b>T2p</b>	<b>T2pp</b>
# Runs	9	7	11	22
Total Time(hrs)	~8.7	~2.8	~5.2	~5.7
#Rollback	2	27	72	145
#Reboot	0	1	2	9
#Lost I/O	0	5	3	10
#Lost Sync	0	1	1	6
	<b>T2d1</b>	<b>T3</b>	<b>T4</b>	<b>T4p</b>
# Runs	3	9	7	3
Total Time(hrs)	~2	~7.9	~5.9	~2.2
#Rollback	12	0	18	7
#Reboot	0	0	1	0
#Lost I/O	0	0	2	1
#Lost Sync	0	0	0	0
	<b>T5</b>	<b>T6</b>	<b>T6p</b>	
# Runs	7	2	7	
Total Time(hrs)	~5.9	~2	~5.5	
#Rollback	16	1	0	
#Reboot	1	1	0	
#Lost I/O	1	0	1	
#Lost Sync	0	0	0	

Table 2: Run Statistics

The total time for each run was then applied to the neutron data and beam spot area to provide a neutron flux for each of the targeting objectives for neutron energies > 1.5 MeV. These are listed in table 3.

The equations are as follows:

$$(2) \quad N = \phi_{fc} \times A_{fc} \times \text{time}$$

N = # of neutrons (integrated)  
 $\phi_f$  = Neutron flux at fission chamber  
 $A_{fc}$  = beam area at fission chamber  
 Time = total time for fission chamber log

$$(3) \quad \phi_{fcc} = N/A_{FWHM}/\text{time}$$

$\phi_{fcc}$  = Neutron flux at FCC  
 N = # of neutrons (integrated)  
 $A_{FWHM}$  = beam area at FCC  
 Time = total time beam shutter open

Objective	Flux (n/cm <sup>2</sup> -s)
T1	8.60E+5
T2	8.81E+5
T2p	8.81E+5
T2pp	6.12E+5
T2d1	6.85E+5
T3	8.81E+5
T4	9.03E+5
T4p	6.23E+5
T5	6.03E+5
T6	6.54E+5
T6p	6.54E+5

Table 3: Neutron Flux

The neutron flux for each objective was then applied to the run statistics to determine the cross sections for each of the system phenomena that were observed. Table 3 lists the cross sections for each of the system phenomena for each of the targeting objectives.

Objective	Cross-Sections (cm <sup>2</sup> )			
	$\sigma_{\text{rollback}}$	$\sigma_{\text{reboot}}$	$\sigma_{\text{I/O}}$	$\sigma_{\text{synch}}$
<b>T1</b>	7.23(+.16)E -11	Not Observed	Not Observed	Not Observed
<b>T2</b>	3.01 (+.33)E -9	1.11(+.42)E -10	5.57 (+.54)E -10	1.11(+.42)E -10
<b>T2p</b>	4.38 (+.30)E -9	1.22(+.25)E -10	1.82 (+.32)E -10	6.08 (+ 1.83)E-11
<b>T2pp</b>	1.18 (+.06)E -8	7.34(+.55)E -10	8.16 (+.39)E -10	4.89(+.38)E -10
<b>T2d1</b>	2.38 (+.05)E -9	Not Observed	Not Observed	Not Observed
<b>T3</b>	Not Observed	Not Observed	Not Observed	Not Observed
<b>T4</b>	9.39(+1.34)E -10	5.22(+ 1.97)E -11	1.44(+.26)E -10	Not Observed
<b>T4p</b>	1.41(+.42)E -9	Not Observed	2.01(+ 1.16)E -10	Not Observed
<b>T5</b>	1.24(+.06)E -9	7.78(+ 2.94)E -11	7.78(+ 2.94)E -11	Not Observed
<b>T6</b>	2.15(+.15)E -10	2.15(+.15)E -10	Not Observed	Not Observed
<b>T6p</b>	Not Observed	Not Observed	7.63(+ 2.88)E-11	Not Observed

Table 4: Cross sections of system phenomena for each targeting objective

These cross sections are probabilities of occurrence where when applied to any given neutron flux, will give a probable number of occurrences per unit time of these phenomena. These cross sections can be applied directly to normal atmospheric neutron conditions. The equation for the derivation of the cross sections is given as:

$$(4) \quad \sigma = (\# \text{events}/\text{time}) * (1/\phi)$$

To determine the number of events per unit time expected for any given flux:

$$(5) \quad \# \text{Events}/\text{time} = \sigma * \phi$$

### Conclusion

Given the cross sections derived in the previous section, it would appear that the components including and around the processors are the most susceptible to neutron particle effects. It was assumed that the rollbacks, loss of I/O and loss of synchronization between the FCC and the data acquisition equipment were caused by SEUs when not accompanied by voltage spikes or over-current conditions. When they were, it was speculated that perhaps a latch-up condition was encountered.

Operating system reboots were originally thought to be cause directly by SEUs, but after further investigation, it was determined

that these were likely caused by legacy software left in the computer. This software had mechanisms called “strike counters” which kept track of the number of errors that were encountered in various parts of the FCC. When the errors reached certain threshold levels, the system would reboot. Although the reboots were likely caused indirectly by the SEUs, it is hard to quantify these phenomena for each strike counter without knowing precisely what causes each.

The results of this experiment were not compared to result obtain for individual components under the same conditions due to the many variables that exist when performing system level tests. It is hard to differentiate which individual component is the source of errors when targeting large groups of components. In addition, as the neutrons passed through the FCC, they were scattered and attenuated in ways that are hard to quantify for any given run. Also, it should be mentioned that the entire FCC computer was not totally immersed in the neutron beam due to difficulty in maintaining and measuring the intensity distribution across the entire computer.

### **Acknowledgements**

This work was performed by members from NASA Langley Research Center Old Dominion University and by members under contract by NASA Langley Research Center from various other companies with support from members at Honeywell, Inc and Los Alamos National Laboratory. A special thanks from the author should go to Celeste Belcastro, PhD, Kenneth Eure, PhD and Dan Koppen of NASA Langley Research Center for providing the opportunity and support necessary for the completion of this research. In addition a special thanks to Boyd Hill and Ed Hogge for providing a means to sift through the many gigabytes of data necessary for this research, and providing it in a very timely fashion.

## REFERENCES

1. D. Binder, E.C. Smith, A.B. Holman, "Satellite anomalies from galactic cosmic rays," *IEEE Trans. on Nuclear Science*, vol. NS-22, no. 6, pp. 2675-2680, Dec. 1975.
2. J. F. Ziegler and W. A. Lanford, "Effect of Cosmic Rays on Computer Memories", *Science*, Vol. 206, pp. 776, 1979.
3. A. Taber and E. Normand, "Investigation and Characterization of SEU Effects and Hardening Strategies in Avionics", IBM Report 92-L75-020-2, Aug. 1992, republished as DNA-Report DNA-TR-94-123, Defense Nuclear Agency, Feb. 1995.
4. Normand, E., and T. J. Baker, 1993, 'Altitude and Latitude Variations in Avionics SEU and Atmospheric Neutron Flux,' *IEEE Trans. Nuclear Science*, vol. 40, no. 6, pp. 1484-1490.
5. Eure, K, Belcastro, C, Hess, R, Vahala, L, Ferguson, M, "Closed-Loop Neutron Particle Effects on a Recoverable Flight Control Computer", Digital Avionics Systems Conference (DASC), Oct. 200
6. <http://home.fujifilm.com/products/science/ip/index.html>, last opened 03/20/2005